

# Topological quantum phase transition and the Berry phase near the Fermi surface in hole-doped quantum wells

BIN ZHOU<sup>1,2</sup>, CHAO-XING LIU<sup>3</sup> and SHUN-QING SHEN<sup>1</sup>

<sup>1</sup> *Department of Physics, and Center for Theoretical and Computational Physics, The University of Hong Kong Pokfulam Road, Hong Kong, China*

<sup>2</sup> *Department of Physics, Hubei University - Wuhan 430062, China*

<sup>3</sup> *Department of Physics and Center for Advanced Study, Tsinghua University - Beijing 100084, China*

received 15 May 2007; accepted in final form 29 June 2007  
published online 25 July 2007

PACS 73.43.Nq – Quantum phase transitions  
PACS 03.65.Vf – Phases: geometric; dynamic or topological  
PACS 72.25.Dc – Spin polarized transport in semiconductors

**Abstract** – We propose a topological quantum phase transition for quantum states with different Berry phases in hole-doped III-V semiconductor quantum wells with bulk and structure inversion asymmetry. The Berry phase of the occupied Bloch states can be characteristic of topological metallic states. It is found that the adjustment of the thickness of the quantum well may cause a transition of the Berry phase in a two-dimensional hole gas. Correspondingly, the jump of the spin Hall conductivity accompanies the change of the Berry phase. This property is robust against the impurity potentials in the system. Experimental detection of this topological quantum phase transition is discussed.

Copyright © EPLA, 2007

**Introduction.** – Topological properties of electron bands or Bloch states are fundamentally important in characterizing the quantum transverse transport of electrons in metals and semiconductors. Studies of the quantum Hall effect reveal the topological origin of quantum Hall conductivity and the existence of novel quantum states of matter [1]. Thouless *et al.* [2] found that quantum Hall conductivity can be expressed in terms of the Chern-Simon number of electron bands. Renewed interest in the anomalous Hall effect leads to an interpretation of “anomalous velocity” in the Karplus-Luttinger formula for anomalous Hall conductivity as an integration of Berry curvatures of occupied Bloch states, which gives a geometric insight of intrinsic contribution in ferromagnetic metals or semiconductors [3,4]. It was also noticed that the Berry phase or Chern-Simon number may have very close relation to the intrinsic and quantum spin Hall effect [5–7]. Very recently, Bernevig *et al.* proposed a topological quantum phase transition of topological insulators in HgTe quantum wells [8].

The Berry phase is acquired by a quantum state upon being transported adiabatically around a loop in the parameter space [9]. It reflects the topological properties of bulk quantum states. Spin-orbit coupling in semiconductors mixes electron Bloch states in the  $k$  space with spin

degrees of freedom. In some two-dimensional (2D) systems the Berry phase is well defined for some band structures near the Fermi surface such as the system with Rashba or Dresselhaus spin-orbit coupling [5]. In this paper, we investigate the quantum size effect of the Berry phase near the Fermi surface of heavy holes in the III-V semiconductor quantum wells with bulk and structure inversion asymmetry, and propose a topological quantum phase transition for topological metallic states with different Berry phases when changing the thickness of the quantum well. The anomaly or discontinuity of quantum transverse transport of electron can be characteristic of this topological quantum phase transition. As examples we study the spin Hall conductance of the systems, and find that the spin Hall conductivity has a jump near the transition point. This property is robust against the impurity scattering and expected to be observed with the current experimental technique.

**Model.** – Consider a [001]-grown 2D quantum well of hole-doped III-V semiconductors. We start with the model Hamiltonian for the valence band near the  $\Gamma$  point in the  $k$  space [10,11],

$$H_{\text{bulk}} = H_L + H_D + H_R. \quad (1)$$

$H_L$  is the Luttinger Hamiltonian [12]

$$H_L = \left( \gamma_1 + \frac{5}{2} \gamma_2 \right) \frac{\hbar^2 k^2}{2m} - \frac{\gamma_2}{m} \hbar^2 (\mathbf{k} \cdot \mathbf{S})^2, \quad (2)$$

where  $\gamma_1, \gamma_2$  are the material parameters,  $k^2 = k_x^2 + k_y^2 + k_z^2$ ,  $m$  is the free electron mass, and  $\mathbf{S} = (S_x, S_y, S_z)$  are  $4 \times 4$  matrices corresponding to spin 3/2.  $H_D$  is the Dresselhaus spin-orbit coupling caused by the bulk inversion asymmetry (BIA) [13]

$$H_D = -\frac{\gamma}{\eta} [k_x (k_y^2 - k_z^2) S_x + \text{c.p.}], \quad (3)$$

where c.p. stands for cyclic permutation of all indices ( $x, y, z$ ),  $\gamma$  is due to bulk inversion asymmetry,  $\eta = \Delta_{so}/(E_g + \Delta_{so})$ ,  $\Delta_{so}$  is the split-off gap energy,  $E_g$  is the band gap energy.  $H_R$  is the Rashba spin-orbit coupling term arising from structure inversion asymmetry (SIA) due to an asymmetry confining potential [14]

$$H_R = \alpha (\mathbf{k} \times \mathbf{S}) \cdot \mathbf{e}_z, \quad (4)$$

where  $\alpha$  is a material parameter [15] and  $\mathbf{e}_z$  is the growth direction of the quantum well.

For a 2D quantum well with finite thickness  $d$ , the first heavy- and light-hole bands have approximate relations of  $\langle k_z \rangle = 0$  and  $\langle k_z^2 \rangle \simeq (\pi/d)^2$ . If the thickness of the quantum well is thin enough, the heavy hole (HH) and light hole (LH) bands are well separated. In this paper, we limit our discussion to the case in which only the first HH band is significantly occupied. By means of the projection perturbation method [16,17], the bulk Hamiltonian, eq. (1), is projected into the space of heavy holes,

$$\begin{aligned} H_{hh} = & \frac{\hbar^2 k^2}{2m_{hh}} + \lambda_1 k^2 (k_- \sigma_+ + k_+ \sigma_-) \\ & + \lambda_2 (k_+^3 \sigma_+ + k_-^3 \sigma_-) + i\lambda_3 (k_-^3 \sigma_+ - k_+^3 \sigma_-) \\ & + i\lambda_4 k^2 (k_+ \sigma_+ - k_- \sigma_-), \end{aligned} \quad (5)$$

where  $\sigma_\alpha$  are the Pauli matrices,  $\sigma_\pm = (\sigma_x \pm i\sigma_y)/2$ ,  $k_\pm = k_x \pm ik_y$ ,

$$\lambda_1 = \frac{3\gamma}{4\eta} \left( 1 - \frac{3m^2 \alpha^2}{4\hbar^4 \gamma_2^2 \langle k_z^2 \rangle} \right), \quad \lambda_2 = \frac{3m^2 \gamma^3 \langle k_z^2 \rangle}{16\hbar^4 \gamma_2^2 \eta^3}, \quad (6)$$

$$\lambda_3 = \frac{3\alpha}{4 \langle k_z^2 \rangle} \left( 1 - \frac{m^2 \alpha^2}{4\hbar^4 \gamma_2^2 \langle k_z^2 \rangle} \right), \quad \lambda_4 = \frac{9m^2 \alpha \gamma^2}{16\hbar^4 \gamma_2^2 \eta^2}, \quad (7)$$

and the effective HH mass  $m_{hh} = m[\gamma_1 + \gamma_2 - 3m^2(\alpha^2 + \beta^2 + 2\alpha\beta \sin 2\theta)/(4\hbar^4 \langle k_z^2 \rangle \gamma_2)]^{-1}$ , with  $\beta = \gamma \langle k_z^2 \rangle / \eta$ . The band mixing between the light and heavy holes is taken into account as the effective spin-orbit couplings. Correspondingly, the projected spin operator  $S_z$  has the form,  $S_{hh}^z = [3/2 - 3m^2(\alpha^2 + \beta^2 + 2\alpha\beta \sin 2\theta)k^2 / (16\hbar^4 \langle k_z^2 \rangle^2 \gamma_2^2)] \sigma_z$ . As a result, there are four types of effective cubic spin-orbit coupling.  $\lambda_1, \lambda_2$ , and  $\lambda_3$  can be adjusted by the thickness  $d$  of the quantum well through  $\langle k_z^2 \rangle$ , and  $\lambda_4$  is determined by the material parameters.

Table 1: Material parameters of selected III-Vs and calculated critical thickness  $d_{c1}$ .

	GaAs	InAs	GaSb	InSb	InP
$E_g$ (eV)	1.519	0.418	0.813	0.237	1.423
$\Delta_{so}$ (eV)	0.341	0.38	0.75	0.81	0.110
$\gamma_1$	6.85	20.4	13.3	37.1	4.95
$\gamma_2$	2.1	8.3	4.4	16.5	1.65
$\gamma$ (eV.Å <sup>3</sup> )	28	130	187	226.8	8.5
$d_{c1}$ (nm)	1.50	0.68	1.83	0.37	1.48

**The Berry phase.** – Now we come to discuss the topological properties of band structure and their quantum-size effect. The effective  $2 \times 2$  Hamiltonian (5) can be diagonalized exactly in the  $k$  space. The two eigenstates are

$$|k, +\rangle = \frac{1}{\sqrt{2}} \begin{pmatrix} 1 \\ e^{i\varphi} \end{pmatrix}, \quad |k, -\rangle = \frac{1}{\sqrt{2}} \begin{pmatrix} e^{-i\varphi} \\ -1 \end{pmatrix}, \quad (8)$$

where  $\varphi$  is given by

$$\tan \varphi = \frac{\lambda_1 \sin \theta - \lambda_2 \sin 3\theta - \lambda_3 \cos 3\theta - \lambda_4 \cos \theta}{\lambda_1 \cos \theta + \lambda_2 \cos 3\theta + \lambda_3 \sin 3\theta - \lambda_4 \sin \theta}, \quad (9)$$

and  $\tan \theta = k_y/k_x$ .

*The case without SIA.* We first only consider the case of the pure BIA, *i.e.*,  $\alpha = 0$ . In this case  $\lambda_3 = \lambda_4 = 0$ , and  $\lambda_1 = 3\gamma/(4\eta)$ ,  $\lambda_2 = 3m^2 \gamma^3 \langle k_z^2 \rangle / (16\hbar^4 \gamma_2^2 \eta^3)$ . Thus, the two-band effective Hamiltonian is reduced to

$$\begin{aligned} H'_{hh} = & \frac{\hbar^2 k^2}{2m_{hh}} + \lambda_1 k^2 (k_- \sigma_+ + k_+ \sigma_-) \\ & + \lambda_2 (k_+^3 \sigma_+ + k_-^3 \sigma_-), \end{aligned} \quad (10)$$

where  $m_{hh} = m[\gamma_1 + \gamma_2 - 3m^2 \beta^2 / (4\hbar^4 \langle k_z^2 \rangle \gamma_2)]^{-1}$ .  $\lambda_1$  is independent of the thickness  $d$ , but  $\lambda_2$  is proportional to  $1/d^2$ . There exists a critical thickness  $d_{c1}$  such that  $\lambda_1 = \lambda_2$ . The value of the critical thickness  $d_{c1} = m\pi\gamma / (2\hbar^2 \gamma_2 \eta)$ , which is determined by material-specific parameters. Table 1 gives material parameters of some III-V semiconductors (after refs. [16,18]) and calculated critical thickness  $d_{c1}$ .

The two dispersion relations corresponding to the eigenstates (8) are

$$E_\mu(k, \theta) = \frac{\hbar^2 k^2}{2m_{hh}} + \mu \lambda(\theta) k^3, \quad (11)$$

where  $\mu = \pm 1$  and  $\lambda(\theta) = \sqrt{\lambda_1^2 + \lambda_2^2 + 2\lambda_1 \lambda_2 \cos 4\theta}$ . In general the two bands do not crossover except at  $k = 0$ . In the case of  $\lambda_1 = \lambda_2$ , *i.e.*, at the critical point of  $d = d_{c1}$ , the two bands become degenerate at  $\theta = \pm\pi/4$  and  $\pm 3\pi/4$ . The Fermi surfaces and dispersion relations along the [110] axis are plotted in fig. 1 for three cases at or near the critical point of  $\lambda_1 = \lambda_2$ . We note that the validity of the above model is restricted to sufficiently

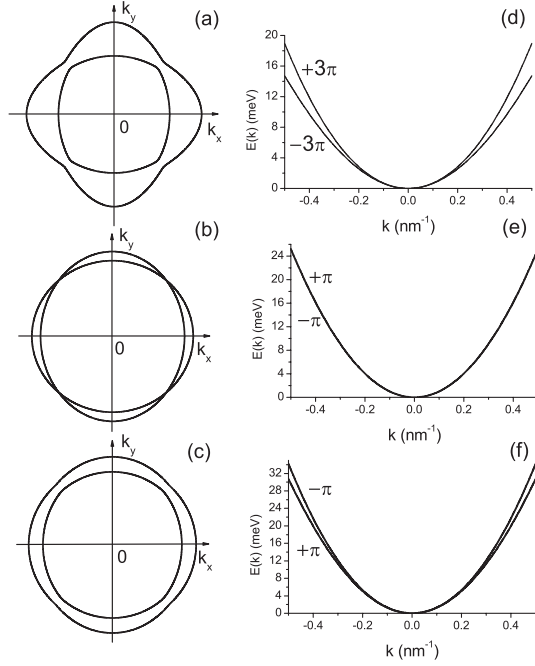


Fig. 1: Fermi surfaces and dispersion branches of heavy hole along the [110] direction for different thicknesses  $d$  of the GaAs quantum well. (a) Fermi surface for  $d < d_{c1}$ ; (b) Fermi surface for  $d = d_{c1}$ ; (c) Fermi surface for  $d > d_{c1}$ ; (d) dispersion branches along the [110] direction for  $d < d_{c1}$ ; (e) dispersion branches along the [110] direction for  $d = d_{c1}$ ; (f) dispersion branches along the [110] direction for  $d > d_{c1}$ . The material parameters of GaAs are given in table 1.  $\pm\pi, \pm 3\pi$  stand for Berry phases.

small wave numbers and hole densities, which is similar to the case of the cubic Rashba model [19].

The topological property of the hole band is revealed by the vector potential for the Berry phase in the  $k$  space,

$$\begin{aligned} \mathbf{A}_\mu &= i \langle k, \mu | \nabla_{\mathbf{k}} | k, \mu \rangle \\ &= -\frac{\mu}{2k} \frac{\lambda_1^2 - 3\lambda_2^2 - 2\lambda_1\lambda_2 \cos 4\theta}{\lambda_1^2 + \lambda_2^2 + 2\lambda_1\lambda_2 \cos 4\theta} \mathbf{e}_\theta. \end{aligned} \quad (12)$$

The associated Berry curvature is  $\nabla_{\mathbf{k}} \times \mathbf{A}_\mu = \gamma_\mu \delta(\mathbf{k}) \mathbf{e}_z$ , where

$$\gamma_\mu = \mu \left[ \pi - 2\pi \frac{(\lambda_1^2 - \lambda_2^2)}{|\lambda_1^2 - \lambda_2^2|} \right], \quad (13)$$

for  $\lambda_1 \neq \lambda_2$  and  $\mu\pi$ , for  $\lambda_1 = \lambda_2$ . The phases are opposite for the two bands. The singularity at  $\mathbf{k} = 0$  indicates the existence of the Berry phase flux or 2D magnetic monopole in the  $k$  space. We notice that the two types of spin-orbit coupling in eq. (10) have quite different contributions to the Berry phase. When the first term dominates  $\lambda_1 > \lambda_2$ ,  $\gamma_\mu = -\mu\pi$  and oppositely  $\gamma_\mu = \mu 3\pi$ . At the critical point of  $\lambda_1 = \lambda_2$ ,  $\gamma_\mu = \mu\pi$ . According to Stokes' theorem,  $\gamma_\mu$  is exactly the Berry phase [9]<sup>1</sup>, which

<sup>1</sup> $\mathbf{A}_\mu$  has the so-called ‘‘gauge choice’’. The gauge we choose is consistent with the following approach: firstly, we add a term  $h\sigma_z$  to the Hamiltonian (5) to lift the degeneracy at  $\mathbf{k} = 0$ , then calculate the Berry phase through the surface integral of the gauge-invariant Berry curvature and take the limit of  $h \rightarrow 0$  at the last step.

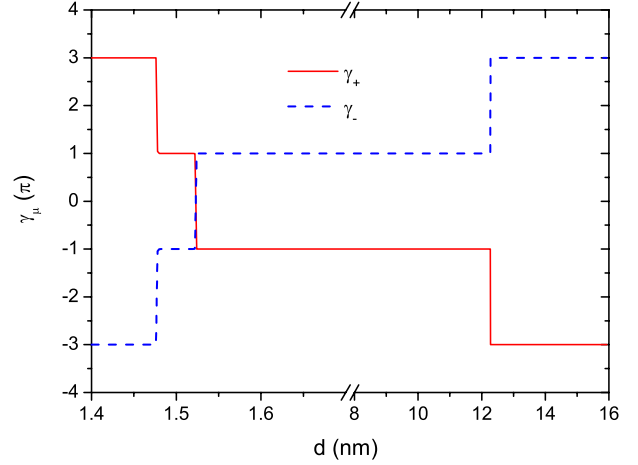


Fig. 2: (Colour on-line) Variation of the Berry phase  $\gamma_\mu$  with the thickness  $d$  of the GaAs quantum well with BIA and SIA. The material parameters are given in the text. The solid line (red) corresponds to  $\gamma_+$ ; the dashed line (blue) to  $\gamma_-$ .

is acquired by a state upon being transported around an arbitrary loop  $C$  including the origin of  $\mathbf{k} = 0$  in the  $k$  space,  $\gamma_\mu = \oint_C d\mathbf{k} \cdot \mathbf{A}_\mu$ . From these results, it indicates that adjustment of the thickness  $d$  near the critical point  $d_{c1}$  may change the value of  $\lambda_2$ , and further causes a change of Berry phase from  $\gamma_\mu = -\mu\pi$  to  $\gamma_\mu = \mu 3\pi$  in the system or vice versa. Since this Berry phase reflects the global topological properties of hole bands in the  $k$  space, it is believed that this phase transition is topological.

*The case with BIA and SIA.* Now we will consider the system with both BIA and SIA. In the following, we use material parameters of III-V semiconductor GaAs given in table 1, and take  $\alpha = 0.01$  eV nm. The variation of the Berry phase  $\gamma_\mu$  with the thickness  $d$  is plotted in fig. 2. Due to SIA, a new step of the Berry phase appears near 1.5 nm. Furthermore, with the increase of the thickness the Berry phase can transit from  $\gamma_\mu = -\mu\pi$  to  $\gamma_\mu = -\mu 3\pi$  at  $d = 12.3$  nm.

Though there exist several transition points of the Berry phase, in the following discussion, we focus on the regime near the transition at  $d_{c2} = 12.3$  nm. In this regime  $\lambda_1$  and  $\lambda_3$  are much larger than  $\lambda_2$  and  $\lambda_4$ . For simplification, we neglect  $\lambda_2$  and  $\lambda_4$ , and the effective Hamiltonian is

$$\begin{aligned} \tilde{H}_{hh} &= \frac{\hbar^2 k^2}{2m_{hh}} + \lambda_1 k^2 (k_- \sigma_+ + k_+ \sigma_-) \\ &\quad + i\lambda_3 (k_-^3 \sigma_+ - k_+^3 \sigma_-). \end{aligned} \quad (14)$$

The two dispersion relations have the same forms as eq. (11) with  $\lambda(\theta) = \sqrt{\lambda_1^2 + \lambda_3^2 + 2\lambda_1\lambda_3 \sin 2\theta}$ . In general the two bands do not crossover except at  $k = 0$ . In the case of  $\lambda_1 = \lambda_3$ , or  $d = d_{c2}$  ( $d_{c2}$  shifts to 12.1 nm due to the ignorance of  $\lambda_2$  and  $\lambda_4$  and remaining the definition of  $\lambda_1$  and  $\lambda_3$  in eqs. (6) and (7)), the two bands become degenerate at  $\theta = 3\pi/4$  and  $7\pi/4$ . The Fermi surfaces are plotted in fig. 3 at or near the critical point of  $\lambda_1 = \lambda_3$ .

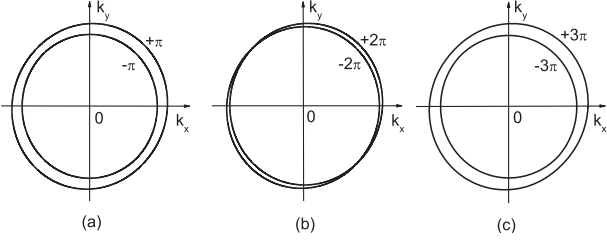


Fig. 3: Fermi surfaces for different thicknesses  $d$  of the GaAs quantum well. (a) Fermi surface for  $d < d_{c2}$ ; (b) Fermi surface for  $d = d_{c2}$ ; (c) Fermi surface for  $d > d_{c2}$ .  $\pm\pi$ ,  $\pm 2\pi$ , and  $\pm 3\pi$  stand for Berry phases.

In this case the vector potential for the Berry phase in the  $k$  space is given as

$$\mathbf{A}_\mu = -\frac{\mu}{2k} \frac{\lambda_1^2 + 3\lambda_3^2 + 4\lambda_1\lambda_3 \sin 2\theta}{\lambda_1^2 + \lambda_3^2 + 2\lambda_1\lambda_3 \sin 2\theta} \mathbf{e}_\theta, \quad (15)$$

and thus the Berry phase is

$$\gamma_\mu = -\mu \left[ 2\pi - \pi \frac{\lambda_1^2 - \lambda_3^2}{|\lambda_1^2 - \lambda_3^2|} \right], \quad (16)$$

for  $\lambda_1 \neq \lambda_3$  and  $-\mu 2\pi$ , for  $\lambda_1 = \lambda_3$ . It follows that the adjustment of the thickness  $d$  may cause a transition of the Berry phase from  $\gamma_\mu = -\mu\pi$  to  $\gamma_\mu = -\mu 3\pi$  in the system or vice versa.

On the other hand, we note that the strength of  $\alpha$  is another parameter which can be modified by a gate field. If the thickness  $d$  of the quantum well is fixed, a change of  $\alpha$  can also induce a change of Berry phase: for example for a GaAs quantum well with  $d = 10$  nm, the critical value  $\alpha_c = 0.014$  eV nm at which the Berry phase can vary from  $\gamma_\mu = -\mu\pi$  to  $\gamma_\mu = -\mu 3\pi$ .

**The topological quantum phase transition and discontinuity of spin Hall conductance.** – The free-electron gas described by the effective Hamiltonian is obviously metallic. The spin-orbit coupling makes the electrons near the Fermi surface to possess different topological properties in the  $k$  space. The question is whether these metallic states with different Berry phases are different from each other such that the Berry phase can be characteristic of these quantum metallic states. To reveal the relevant physical properties of these metallic states, we study the spin Hall effect of this system, which has attracted a lot of interests in recent years [20,21]. Without loss of generality, we shall focus on the effective Hamiltonian in eq. (14) to explore the physical consequence of the change of the Berry phase near  $d_{c2}$ . The other two transition points of the Berry phase require much thinner thickness.

For a realistic calculation we need to consider the effect of impurities, which has drastic influence on some systems such as the linear Rashba system [21,22]. For simplicity, we consider  $\tilde{H}_{hh}$  in eq. (14) with nonmagnetic impurities with short-ranged potential:  $V(\mathbf{r}) = V_0 \sum_i \delta(\mathbf{r} - \mathbf{R}_i)$ , where  $V_0$

is the strength of the impurities. The retarded Green function can be written as  $G^R(\mathbf{k}, E, \Sigma^R) = (E - \tilde{H}_{hh} - \Sigma^R)^{-1}$ , where the self-energy  $\Sigma^R$  is obtained in the Born approximation by solving the self-consistent equation,

$$\Sigma^R = n_i V_0^2 \int \frac{d\mathbf{k}}{(2\pi)^2} G^R(\mathbf{k}, E, \Sigma^R), \quad (17)$$

where  $n_i$  is the density of the impurity. In this problem, the self-energy has a diagonal form,  $\Sigma^R = \xi^R \mathbf{I}$ , with  $\mathbf{I}$  being the  $2 \times 2$  unit matrix. The spin current operator  $J_y^z$  is defined as  $J_y^z = (\hbar/2)\{v_y, S_{hh}^z\}$ , and the velocity operators are  $v_x \equiv [x, \tilde{H}_{hh}]/(i\hbar)$  and  $v_y \equiv [y, \tilde{H}_{hh}]/(i\hbar)$ . To calculate the linear response of spin current to the dc electric field, we take the vertex correction [22], and the spin Hall conductivity reads

$$\sigma_{yx}^z = \frac{e\hbar}{2\pi} \int \frac{d\mathbf{k}}{(2\pi)^2} \text{Tr}_\sigma [J_y^z G^R \mathbf{V}_x G^A], \quad (18)$$

where  $\mathbf{V}_x$  is the velocity operator with the vertex correction. The self-consistent vertex equation includes the diagrams with impurity ladders into the vertex part [23]

$$\mathbf{V}_x = v_x + n_i V_0^2 \int \frac{d\mathbf{k}}{(2\pi)^2} G^R \mathbf{V}_x G^A. \quad (19)$$

The solution of  $\mathbf{V}_x$  has the form  $\mathbf{V}_x = v_x + \sum_i c_i \sigma_i$ , and can be determined self-consistently. The detailed calculation gives the solution  $c_z = 0$  and

$$c_x = \frac{A_a A_d + A_b A_{10}}{A_c A_d - A_{10}^2}, \quad c_y = \frac{A_a A_{10} + A_b A_c}{A_c A_d - A_{10}^2}, \quad (20)$$

where  $A_a = A_1 + A_2 + A_3$ ,  $A_b = A_4 + A_5 + A_6$ ,  $A_c = 1 - A_7 - A_8$ , and  $A_d = 1 - A_7 - A_9$ . The relevant parameters are

$$A_i = \frac{n_i V_0^2}{4} \sum_{\mu, \nu} \int \frac{d\mathbf{k}}{(2\pi)^2} \Gamma_i^{\mu\nu} G_\mu^R G_\nu^A, \quad (21)$$

where

$$G_\mu^{R(A)} = \frac{1}{E - E_\mu - \xi^{R(A)}}, \quad (22)$$

$$\Gamma_1^{\mu\nu} = \frac{(\mu + \nu)\kappa_x}{\kappa} \frac{\partial \varepsilon}{\hbar \partial k_x}, \quad \Gamma_2^{\mu\nu} = (1 - \mu\nu) \frac{\partial \kappa_x}{\hbar \partial k_x}, \quad (23)$$

$$\Gamma_3^{\mu\nu} = \frac{\mu\nu\kappa_x}{\kappa} \frac{\partial \kappa}{\hbar \partial k_x}, \quad \Gamma_4^{\mu\nu} = \frac{(\mu + \nu)\kappa_y}{\kappa} \frac{\partial \varepsilon}{\hbar \partial k_x}, \quad (24)$$

$$\Gamma_5^{\mu\nu} = (1 - \mu\nu) \frac{\partial \kappa_y}{\hbar \partial k_x}, \quad \Gamma_6^{\mu\nu} = \frac{\mu\nu\kappa_y}{\hbar \kappa} \frac{\partial \kappa}{\partial k_x}, \quad (25)$$

$$\Gamma_7^{\mu\nu} = 1 - \mu\nu, \quad \Gamma_8^{\mu\nu} = \frac{2\mu\nu\kappa_x^2}{\kappa^2}, \quad (26)$$

$$\Gamma_9^{\mu\nu} = \frac{2\mu\nu\kappa_y^2}{\kappa^2}, \quad \Gamma_{10}^{\mu\nu} = \frac{2\mu\nu\kappa_x\kappa_y}{\kappa^2}, \quad (27)$$

with  $\kappa_x = k_x k^2 \lambda_1 - k_y (k_y^2 - 3k_x^2) \lambda_3$ ,  $\kappa_y = k_y k^2 \lambda_1 - k_x (k_x^2 - 3k_y^2) \lambda_3$ ,  $\kappa^2 = \kappa_x^2 + \kappa_y^2$ , and  $\varepsilon = \hbar^2 k^2 / (2m_{hh})$ . Using the self-consistent solution of self-energies in eq. (17), we can calculate the spin Hall conductivity explicitly.

For numerical calculation here we adopt the material parameters of GaAs given above and the Fermi energy  $E_f = 2.5$  meV which is close to the bottom of the bands.

Before doing the numerical calculation, we first consider the problem in the clean limit. The vertex-corrected velocity consists of two parts, the bare velocity  $v_x$  and vertex correction  $\delta v_x = c_x \sigma_x + c_y \sigma_y$ . Correspondingly, the spin Hall conductivity in eq. (18) can be divided into the intrinsic part and the vertex correction part. Denote by  $\tau^{-1} = -\frac{2}{\hbar} \text{Im}(\xi^R)$  the life time. In the clean limit of  $n_i \rightarrow 0$ ,  $\tau \rightarrow +\infty$ , the intrinsic part of spin Hall conductivity gives

$$\sigma_{yx}^{z,int} = \frac{3e\hbar^2}{16\pi^2} \int \frac{\sin^2 \theta d\theta}{m_{hh}\lambda^3} \left( \frac{1}{k_f^-} - \frac{1}{k_f^+} \right) \times (\lambda_1^2 + 3\lambda_3^2 + 4\lambda_1\lambda_3 \sin 2\theta), \quad (28)$$

where  $k_f^\pm(\theta)$  are  $\theta$ -dependent Fermi momenta of two bands. This can be also obtained from the Kubo formula explicitly. In the low density of carriers,  $1/k_f^- - 1/k_f^+ \approx -2m_{hh}\lambda(\theta)/\hbar^2$ . Using this formula, we reach an explicit relation between the intrinsic part of the spin Hall conductivity and the Berry phase near the Fermi surface:

$$\sigma_{yx}^{z,int} = \frac{3e}{16\pi^2} \sum_{\mu} \mu \gamma_{\mu}(d). \quad (29)$$

A similar relation has already been obtained for the system with the Rashba and Dresselhaus spin-orbit coupling, once the two conduction bands are occupied simultaneously [5,6]. This relation reflects the close relation between the spin Hall conductance and the topological properties of the Fermi surface. Taking into account the vertex correction, the total spin Hall conductivity in the clean limit is

$$\sigma_{yx}^z = -\frac{3e}{8\pi} \left[ 1 - \frac{\hbar}{k_f^2 \lambda_1} \left( c_x + \frac{\lambda_3}{\lambda_1} c_y \right) \right], \quad (30)$$

for  $\lambda_1 > \lambda_3$  (with  $k_f = (k_f^+ + k_f^-)/2$  independent of  $\theta$ ) and  $\sigma_{yx}^z = -9e/(8\pi)$ , for  $\lambda_1 < \lambda_3$  (see footnote <sup>2</sup>). The parameters  $c_x$  and  $c_y$  can be calculated numerically, and the result is plotted in fig. 4.

Unlike the 2D Rashba system in which the intrinsic spin Hall conductivity can be suppressed by the vertex correction completely [22,24], the spin Hall conductivity in the present system can survive in the clean limit. In the case of  $\lambda_1 > \lambda_3$  the vertex correction almost cancels the intrinsic part when the system deviates from the transition point,  $\sigma_{yx}^z \approx +0.5e/(8\pi)$  but has a large residue near the transition point. In the case of  $\lambda_1 < \lambda_3$  the vertex correction is zero, which is consistent with previous calculations by Murakami [25] and Bernevig *et al.* [26]. In

<sup>2</sup> $\sigma_{xy}^z = 9e/(8\pi)$  was already found in ref. [19] where those authors concentrated on the spin-orbit coupling term proportional to  $\lambda_3$ . In fact  $\sigma_{xy}^z = -\sigma_{yx}^z$  (cf. eq. (25) in ref. [19]), thus our result is consistent with that of ref. [19].

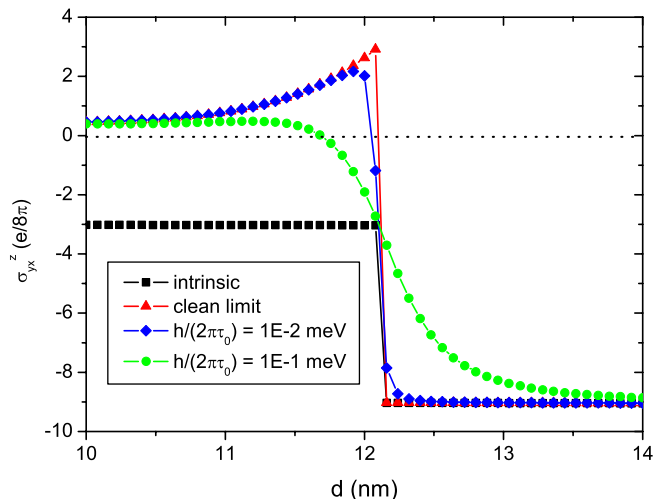


Fig. 4: (Colour on-line) Variation of the spin Hall conductivity  $\sigma_{yx}^z$  with the thickness  $d$  of the GaAs quantum well. The material parameters are given in the text and the given Fermi energy  $E_f$  is equal to 2.5 meV. The squares (black) correspond to the intrinsic part of spin Hall conductivity; the triangle (red) to spin Hall conductivity in the clean limit; the diamonds (blue) to  $\hbar/\tau_0 = 10^{-2}$  meV; the circles (green) to  $\hbar/\tau_0 = 10^{-1}$  meV. Here  $\hbar/\tau_0 = mn_i V_0^2/\hbar^2$ .

general, it has been realized that the symmetries of the spin-dependent part of velocities  $v_j = \partial H/\hbar \partial k_j$  play an essential role in the vertex correction to transverse transport. The parts from the  $\lambda_2$  and  $\lambda_3$  terms have  $d$ -wave symmetry, and have no vertex contribution. The parts from the  $\lambda_1$  and  $\lambda_4$  terms contain two terms of  $s$ - and  $d$ -wave, respectively, where only the term of  $s$ -wave symmetry contributes to the vertex correction.

For a finite density of impurities, numerical results of the total spin Hall conductivity for different life times are plotted in fig. 4. The sharp jump of spin Hall conductivity near the transition point is smeared for the strong disorder effect. As a result, it is concluded that a jump of the intrinsic spin Hall conductivity accompanies the change of the Berry phases near the Fermi surface and it survives after taking into account the disorder effect of impurities. Here we only consider short-range scattering potentials, and it should be noted that the resulting vertex correction will depend in general on the form and in particular the spatial range of the scatterers.

**Discussion and summary.** – From the calculation above, we established a relation between the topological quantum phase transition and spin-resolved quantum transverse transport in the system. The spin Hall effect has been observed experimentally in both  $p$ - and  $n$ -doped semiconductor systems [27,28] and metals such as aluminum [29] and platinum [30]. Especially, the technique of Wunderlich *et al.* [28] can be applied to observe this topological quantum phase transition explicitly. The 2D hole-doped layer of the (Al, Ga)As/GaAs heterojunction is designed as a part of a  $p$ - $n$  junction light-emitting diode

with a specially designed coplanar geometry which allows an angle-resolved polarization detection at opposite edges of the 2D hole system. When an electric field is applied across the hole channel, a nonzero out-of-plane component of the angular momentum can be detected whose magnitude depends on the thickness of the heterojunction for 2D holes. A series of samples with different thickness around  $d_{c2}$  are required to detect the jump near the transition point. On the other hand, as mentioned above, we can also vary the Rashba coupling  $\alpha$  near the critical  $\alpha_c$  by adjusting the gate voltage, and detect the jump of spin accumulation at edges of the 2D hole quantum well with fixed thickness to reveal the transition of the Berry phase. Technically it is believed that there is not any obstacle to observe this transition. In short, the topological quantum phase can be characterized by the Berry phase accumulated by the adiabatic motion of particles on the occupied Bloch states of hole (or electron). The conventional phase transition is characteristic of the discontinuity of the derivative of the free energy with respect to temperature. Instead, this novel type of topological quantum phase transition is revealed by the discontinuity or anomaly of quantum spin transverse transport in the system.

\*\*\*

This work was supported by the Research Grant Council of Hong Kong under Grant No. HKU 7042/06P, and the CRCG of the University of Hong Kong.

## REFERENCES

- [1] PRANGE R. E. and GIRVIN S. M. (Editors), *The Quantum Hall Effect* (Springer-Verlag, New York) 1987.
- [2] THOULESS D. J., KOHMOTO M., NIGHTINGALE M. P. and DEN NIJS M., *Phys. Rev. Lett.*, **49** (1982) 405.
- [3] JUNGWIRTH T., NIU Q. and MACDONALD A. H., *Phys. Rev. Lett.*, **88** (2002) 207208; ONADA M. and NAGAOSA N., *J. Phys. Soc. Jpn.*, **71** (2002) 19; FANG Z., NAGAOSA N., TAKAHASHI K. S., ASAMITSU A., MATHIEU R., OGASAWARA T., YAMADA H., KAMASAKI M., TOKURA Y. and TERAOKA K., *Science*, **302** (2003) 92.
- [4] HALDANE F. D. M., *Phys. Rev. Lett.*, **93** (2004) 206602.
- [5] SHEN S. Q., *Phys. Rev. B*, **70** (2004) 081311(R).
- [6] CHANG M. C., *Phys. Rev. B*, **71** (2005) 085315; CHEN T.-W., HUANG C.-M. and GUO G. Y., *Phys. Rev. B*, **73** (2006) 235309.
- [7] SHENG D. N., WENG Z. Y., SHENG L. and HALDANE F. D. M., *Phys. Rev. Lett.*, **97** (2006) 036808.
- [8] BERNEVIG B. A., HUGHES T. L. and ZHANG S.-C., *Science*, **314** (2006) 1757.
- [9] BERRY M. V., *Proc. R. Soc. London, Ser. A*, **392** (1984) 45.
- [10] MEIER F. and ZAKHARCHENYA B. P. (Editors), *Optical Orientation* (North-Holland, Amsterdam) 1984.
- [11] BULAEV D. V. and LOSS D., *Phys. Rev. Lett.*, **95** (2005) 076805.
- [12] LUTTINGER J. M., *Phys. Rev.*, **102** (1956) 1030.
- [13] DRESSELHAUS G., *Phys. Rev.*, **100** (1955) 580.
- [14] RASHBA E. I., *Fiz. Tverd. Tela (Leningrad)*, **2** (1960) 1224 (*Sov. Phys. Solid State*, **2** (1960) 1109).
- [15] WINKLER R., *Phys. Rev. B*, **62** (2000) 4245; WINKLER R., NOH H., TUTUC E. and SHAYEGAN M., *Phys. Rev. B*, **65** (2002) 155303.
- [16] WINKLER R., *Spin-Orbit Coupling Effects in Two-Dimensional Electron and Hole Systems* (Springer-Verlag, Berlin) 2003.
- [17] ZHU B. F. and CHANG Y. C., *Phys. Rev. B*, **50** (1994) 11932; SHEN S. Q. and WANG Z. D., *Phys. Rev. B*, **61** (2000) 9532; FOREMAN B. A., *Phys. Rev. Lett.*, **84** (2000) 2505.
- [18] MILLER J. B., ZUMBÜHL D. M., MARCUS C. M., LYANDA-GELLER Y. B., GOLDBABER-GORDON D., CAMPMAN K. and GOSSARD A. C., *Phys. Rev. Lett.*, **90** (2003) 076807; DE ANDRADA E SILVA E. A., LA ROCCA G. C. and BASSANI F., *Phys. Rev. B*, **50** (1994) 8523; CARDONA M., CHRISTENSEN N. E. and FASOL G., *Phys. Rev. B*, **38** (1988) 1806.
- [19] SCHLIEMANN J. and LOSS D., *Phys. Rev. B*, **71** (2005) 085308.
- [20] MURAKAMI S., NAGAOSA N. and ZHANG S.-C., *Science*, **301** (2003) 1348; SINOVA J., CULCER D., NIU Q., SINITSYN N. A., JUNGWIRTH T. and MACDONALD A. H., *Phys. Rev. Lett.*, **92** (2004) 126603; SHEN S. Q., MA M., XIE X. C. and ZHANG F. C., *Phys. Rev. Lett.*, **92** (2004) 256603.
- [21] SINOVA J., MURAKAMI S., SHEN S. Q. and CHOI M. S., *Solid State Commun.*, **138** (2006) 214; SCHLIEMANN J., *Int. J. Mod. Phys. B*, **20** (2006) 1015.
- [22] INOUE J. I., BAUER G. E. W. and MOLENKAMP L. W., *Phys. Rev. B*, **70** (2004) 041303(R); KHAETSKII A., *Phys. Rev. Lett.*, **96** (2006) 056602; RAIMONDI R., LEADBEATER M., SCHWAB P., CAROTI E. and CASTELLANI C., *Phys. Rev. B*, **64** (2001) 235110.
- [23] ABRIKOSOV A. A., GORKOV L. P. and DZYALOSHINSKI I. E., *Methods of Quantum Field Theory in Statistical Physics* (Dover, New York) 1963.
- [24] SHEN S. Q., *Phys. Rev. Lett.*, **95** (2005) 187203; ZHOU B., REN L. and SHEN S. Q., *Phys. Rev. B*, **73** (2006) 165303.
- [25] MURAKAMI S., *Phys. Rev. B*, **69** (2004) 241202(R).
- [26] BERNEVIG B. A. and ZHANG S. C., *Phys. Rev. Lett.*, **95** (2005) 016801.
- [27] KATO Y. K., MYERS R. C., GOSSARD A. C. and AWSCHALOM D. D., *Science*, **306** (2004) 1910.
- [28] WUNDERLICH J., KAESTNER B., SINOVA J. and JUNGWIRTH T., *Phys. Rev. Lett.*, **94** (2005) 047204.
- [29] VALENZUELA S. O. and TINKHAM M., *Nature (London)*, **442** (2006) 176.
- [30] KIMURA T., OTANI Y., SATO T., TAKAHASHI S. and MAEKAWA S., *Phys. Rev. Lett.*, **98** (2007) 156601.